

H-atom abstraction from thiols by C-centered radicals. A theoretical and experimental study of reaction rates

Darren L. Reid,^a Gennady V. Shustov,^{†a} David A. Armstrong,^a Arvi Rauk,^{*a}
Man Nien Schuchmann,^b M. Shahid Akhlaq^b and Clemens von Sonntag^{‡b}

^a Department of Chemistry, University of Calgary, Calgary, AB, T2K 1N6, Canada.
E-mail: rauk@ucalgary.ca Tel: +1 403 220 6247

^b Max-Planck-Institut für Strahlenchemie, Stiftstrasse, 34-36, P. O. Box 101365,
D-45470-Mülheim an der Ruhr, Germany. E-mail: Clemens@vonSonntag.de;
Fax: +49 208 306 3951; Tel: +49 208 306 3529

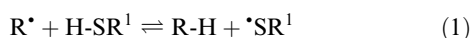
Received 13th November 2001, Accepted 29th January 2002

First published as an Advance Article on the web 17th May 2002

The Arrhenius parameters and rates of reaction of three hydroxyl radicals, methyl radical, and the hindered primary C-centred radical from t-butyl alcohol with dithiothreitol were measured by pulse radiolysis in water. The bimolecular rate constants were found to be in the order: ${}^{\bullet}\text{C}(\text{CH}_3)_2\text{OH} > {}^{\bullet}\text{CH}(\text{CH}_3)\text{OH} > {}^{\bullet}\text{CH}_2\text{OH} > {}^{\bullet}\text{CH}_3 > {}^{\bullet}\text{CH}_2\text{C}(\text{CH}_3)_2\text{OH}$. The reaction of three of these, ${}^{\bullet}\text{C}(\text{CH}_3)_2\text{OH}$, ${}^{\bullet}\text{CH}_2\text{OH}$, and ${}^{\bullet}\text{CH}_3$, with methanethiol were examined at the *ab initio* B3LYP/6311+G(d,p) level, coupled with transition state theory, both in the gas phase and in solution. The solvent effects are evaluated by two different continuum models (SCIPCM, CPCM), coupled with a novel approach to the calculation of the solution phase entropy. The reaction is discussed in terms of the charge and spin polarization in the transition state, as determined by AIM analysis, and in terms of orbital interaction theory. Rate constants, calculated by transition state theory are in good agreement with the experimental data.

1. Introduction

The reaction of carbon-centered radicals with thiols is important to a number of chemical as well as biological processes (eqn. (1)).^{1,2} This reaction is of particular interest due to its role in the repair reaction in biological systems in which a H-atom is donated to a site of oxidative damage. Glutathione, the most abundant free thiol, is generally regarded as the repair agent.³ The cysteine residue also plays a central role in proteins active in oxidation–reduction reactions.^{4,5} In particular H transfer between carbon-centered backbone-based peptide radicals and cysteine S–H groups occurs in class III ribonucleotide reductases.⁶



The limited aqueous phase data available suggest the rate constants for this reaction are almost independent of the oxidative power of the C-centered radicals, or the bond dissociation enthalpy (BDE) of their parents.¹ In fact, the available aqueous phase data indicates that the more stable C-centred radical reacts more rapidly: (k_1 : ${}^{\bullet}\text{C}(\text{CH}_3)_2\text{OH} > {}^{\bullet}\text{CH}(\text{CH}_3)\text{OH} > {}^{\bullet}\text{CH}_2\text{OH}$), although the difference between the slowest and the fastest is less than an order of magnitude.^{7–10} It has been suggested that the reactivity order could be accounted for by a polar transition state requiring some negative charge on sulfur (and therefore some cationic character at C).¹

In this work, the reactions of the α -hydroxy radicals with dithiothreitol, together with ${}^{\bullet}\text{CH}_3$ and ${}^{\bullet}\text{CH}_2\text{C}(\text{CH}_3)_2\text{OH}$, were

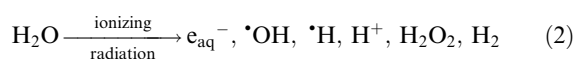
measured by pulse radiolytic techniques. In addition, high level theoretical procedures were applied to the study of hydrogen abstraction from methanethiol ($\text{R}^1 = \text{CH}_3$), according to eqn. (1) by the three radicals: methyl radical ($\text{R} = \text{CH}_3$), hydroxymethyl radical ($\text{R} = \text{CH}_2\text{OH}$), and 2-hydroxy-2-propyl radical ($\text{R} = \text{C}(\text{CH}_3)_2\text{OH}$). Gas and solution phase results are presented and the reactivity is rationalized in terms of the charge polarization in the transition states as evaluated by Atoms-in-Molecules (AIM) theory,¹¹ and by orbital interaction theory.^{12,13}

2. Methods

2.1. Experimental procedures

Rate constants were determined pulse radiolytically.¹⁴ A thermostatted cell allowed us to keep the temperature within ≤ 0.5 K of the desired temperature. Solutions were made up in Milli-Q-filtered (Millipore) water and were saturated with N_2O (Messer Griesheim). All chemicals used in these experiments were commercially available and used without further purification. The pH of the solution was adjusted to 7.5 with phosphate buffer.

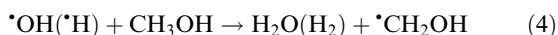
Hydroxyl radicals, solvated electrons and hydrogen atoms are generated in the radiolysis of water (reaction (2)). The radiation-chemical yields (G values) of the primary radicals are $G({}^{\bullet}\text{OH}) \approx G(e_{\text{aq}}^-) = 2.9 \times 10^{-7} \text{ mol J}^{-1}$, $G(\text{H}^{\bullet}) = 0.6 \times 10^{-7} \text{ mol J}^{-1}$, and $G(\text{H}_2\text{O}_2) \approx 0.7 \times 10^{-7} \text{ mol J}^{-1}$. N_2O is used to convert the solvated electron into ${}^{\bullet}\text{OH}$ (reaction (3)).



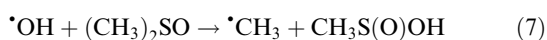
[†] Present address: Department of Chemistry, Simon Fraser University, Burnaby, BC, V5A 1S6, Canada.

[‡] Present address: Institut fuer Oberflaechenmodifizierung (IOM), Permoserstrasse 15, D-04303 Leipzig, Germany.

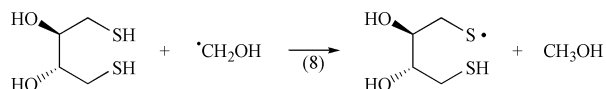
In the presence of a large excess of added alkyl radicals generating substrates over 1,4-dithiothreitol, $\cdot\text{OH}$ and H^\cdot react predominantly with these substrates and only a very minor fraction with 1,4-dithiothreitol (for rate constants see ref. 15). In the case of methanol, they give rise to 95% hydroxymethyl and 5% methoxyl radicals (reactions (4) and (5)).¹⁶ The latter undergo a rapid 1,2-H shift (reaction (6)),¹⁷ *i.e.* the yield of this α -hydroxyalkyl radical is 100%.



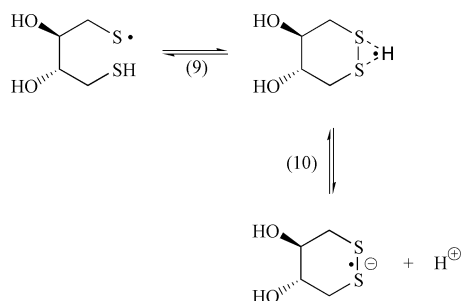
With ethanol and 2-propanol, the yield of α -hydroxyalkyl radicals is close to 85%.¹⁶ With tertiary butanol, 2-hydroxy-2-methylpropyl radicals ($\cdot\text{CH}_2\text{C}(\text{CH}_3)_2\text{OH}$) and some 5% tertiary butoxyl radicals ($(\text{CH}_3)_3\text{CO}^\cdot$) are formed.¹⁶ The latter undergo rapid fragmentation¹⁸ giving rise to acetone and $\cdot\text{CH}_3$. Methyl radicals were generated by reacting dimethylsulfoxide with $\cdot\text{OH}$ (reaction (7)). This reaction yields $\cdot\text{CH}_3$ in 92% yield.¹⁹ The remainder are $\cdot\text{CH}_2\text{S}(\text{O})\text{CH}_3$ radicals formed by H-abstraction.



In the presence of 1,4-dithiothreitol, these alkyl radicals abstract an H atom (*e.g.* reaction (8)).



In this system, the ensuing thiyl radicals rapidly cyclise and deprotonate (equilibria (9) and (10); apparent pK_a at 5.2).²⁰ Experiments have been carried out at pH 7.5 in the presence of low concentrations of phosphate buffer ($\sim 1 \times 10^{-3} \text{ mol dm}^{-3}$) in order to ensure that the equilibrium is shifted to the right.



The disulfide radical anion has a very strong absorption at 390 nm.^{8,20,21} Since equilibria (9) and (10) are rapidly established,²⁰ the rate of build up of the 390 nm absorption monitors the kinetics of the H-abstraction reaction (*e.g.* reaction (8)).

2.2. Theoretical procedures

The *ab initio* calculations presented here were performed using the Gaussian 98 molecular orbital package²² except for the SCIPCM calculations which were run using the Gaussian 94²³ implementation of this method. All calculations including geometry optimizations and frequency calculations, unless stated otherwise, were carried out using the B3LYP hybrid HF-DFT procedure implemented in the Gaussian molecular orbital packages with the 6-311+G(d,p) basis set. This is a triple split basis set with diffuse functions on all heavy atoms and polarization functions on all heavy atoms and hydrogens. The frequencies were scaled by a factor of 0.98 in the calculation of the zero point energy (ZPE) correction, and thermodynamic functions, $(H_{298}^\circ - H_0^\circ)$ and S at 298 K.²⁴ Basis set

superposition error (BSSE) has been found to be relatively small for the B3LYP hybrid functional with large basis sets similar to the one used here, $\sim 1 \text{ kJ mol}^{-1}$, therefore a correction has not been applied.²⁵ Charge and spin distributions were calculated by the AIMPAC¹¹ system of programs.

2.2.1. The reaction profile at 0 K. The reaction shown in eqn. (1) is characterized at three points, corresponding to the structures of the reactants ($\text{CH}_3\text{SH} + \text{C}^\cdot$ radical), the products ($\text{CH}_3\text{S}^\cdot$ radical + parent C-H), and the transition state connecting them. The energies of each of these points are subject to different computational errors due to basis set and correlation effects and therefore some inaccuracy will also be reflected in the relative energies, which are identified with ΔH and ΔH^\ddagger . A measure of the error associated with the energies of the reactants and products, and therefore, with ΔH of reaction (1), may be gained by comparing the calculated BDE with the experimental value, *i.e.*, the heat of reaction (11), D_{AH} .



Thus, for CH_3SH , $D_{\text{SH}}(\text{calc}) = 342.4 \text{ kJ mol}^{-1}$ and $D_{\text{SH}}(\text{exptl}) = 360.6 \text{ kJ mol}^{-1}$.²⁶⁻²⁸ The difference, $\Delta D_{\text{SH}} = 18.1 \text{ kJ mol}^{-1}$, is attributed primarily to $\text{CH}_3\text{S}^\cdot$ (see Fig. 1a). The energy of the right hand side of eqn. (1) is adjusted by this amount. In a parallel manner, ΔD_{CH} values for $\cdot\text{CH}_3$ and $\cdot\text{CH}_2\text{OH}$, 7.3 kJ mol^{-1} and 10.7 kJ mol^{-1} , respectively, may be derived from the parent species: CH_4 ($D_{\text{CH}}(\text{calc}) = 425.4 \text{ kJ mol}^{-1}$, $D_{\text{CH}}(\text{exptl}) = 432.6 \text{ kJ mol}^{-1}$,^{26,27,29}) and CH_3OH ($D_{\text{CH}}(\text{calc}) = 384.9 \text{ kJ mol}^{-1}$, $D_{\text{CH}}(\text{exptl}) = 395.6 \text{ kJ mol}^{-1}$,^{26,27,30,31}) and applied to adjust the energy of the reactant side of eqn. (1) where the C-centred radicals appear. For 2-hydroxy-2-propyl radical, the same value is applied as for hydroxymethyl. In all cases the experimental BDE at 0 K was derived from the available BDE at 298.15 K by applying the calculated $H_{298}^\circ - H_0^\circ$ correction. Evaluation of the reactant

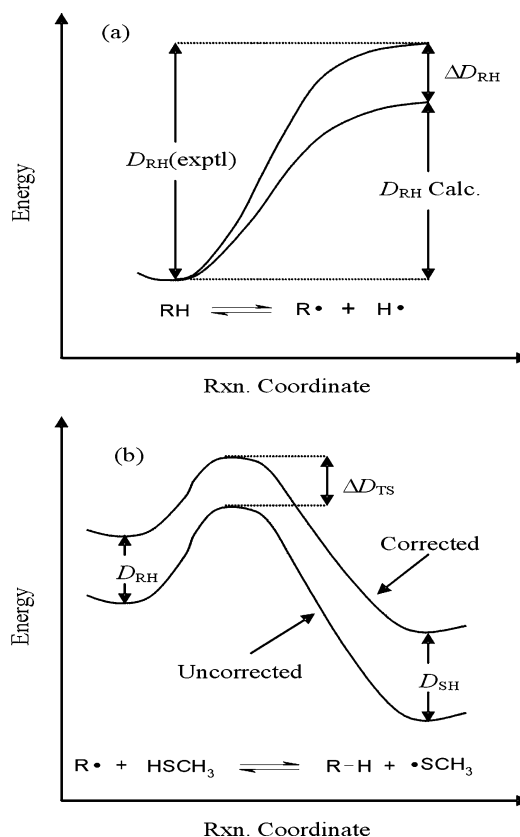


Fig. 1 Experimental correction to the calculated bond dissociation energies (a) and the calculated enthalpies of activation (b).

and product energies in this manner ensures that the heat of eqn. (1), ΔH , is correct at 0 K. In order to improve the accuracy of the enthalpy of activation of eqn. (1), ΔH^\ddagger at 0 K, the correction, ΔD_{TS} , for the transition state, which has both S- and C-radical character, is the weighed average (eqn. (12)),

$$\Delta D_{\text{TS}} = f\Delta D_{\text{C-H}} + (1-f)\Delta D_{\text{S-H}} \quad (12)$$

where f is the fraction of spin remaining on the C-centred-radical part in the transition state. The procedure just described is illustrated in Fig. 1. Spin distributions are discussed below.

2.3. Thermochemical procedures

2.3.1. Rate constants, k . The experimental data to which the calculated results will be evaluated and compared are available as rate constants and Arrhenius parameters for reaction (1) ($\text{R}^1\text{SH} = \text{dithiothreitol}$) in solution. In the thermodynamic formulation of transition state theory (TST), the rate constant for a reaction, k_{TST} , is related to the free energy of activation, ΔG^\ddagger , by the Eyring equation (eqn. (13)):³²

$$k_{\text{TST}} = (k_{\text{B}}T/h)(c^\circ)^{1-m}e^{-\Delta G^\ddagger/RT} \quad (13)$$

where k_{B} and h are Boltzmann's and Planck's constants, respectively, R is the ideal gas constant, c° is the unit molar concentration appropriate for the chosen standard state, and m is the order of reaction. The factor, $(c^\circ)^{1-m}$, provides the correct units for the rate constant of unimolecular and bimolecular reactions. In the present work, free energies are determined for two standard states, both at 298 K: in the gas phase, the pressure is 1 atm, and $c^\circ = 0.0408 \text{ mol dm}^{-3}$; in solution, $c^\circ = 1.0 \text{ mol dm}^{-3}$. A tunnelling correction, κ , due to Wigner,^{33–35} is applied.

$$\kappa \approx 1 + \frac{1}{24} \left(\frac{h\nu^\ddagger}{k_{\text{B}}T} \right)^2 \quad (14)$$

where ν^\ddagger is the magnitude of the imaginary frequency of motion along the reaction coordinate at the transition state. Thus, the rate constant, k , is given by eqn. (15),

$$k = \kappa k_{\text{TST}} \quad (15)$$

In the following sections the procedures for calculating the gas phase free energy of activation ($\Delta G_{(\text{g})}^\ddagger$) which will be used in the evaluation of the rate constants are presented first, followed by the necessary modifications to the gas phase results in order to obtain the aqueous phase free energy of activation ($\Delta G_{(\text{aq})}^\ddagger$).

2.3.2. Gas phase thermochemistry. The values of $H_{298}^\circ - H_0^\circ$ required to obtain heats of reaction and activation at 298 K and the entropies, S , needed in the evaluation of the free energies of reaction and activation were calculated by standard statistical thermodynamic methods, based on the rigid rotor-harmonic oscillator model.³⁶ All torsional motions were treated as vibrations with one exception. For the intermolecular hydrogen transfer transition states the lowest real frequency normal mode, corresponding to torsion about the line connecting the migrating hydrogen, was treated as a free rigid rotation. In the treatment of enthalpies and entropies, as discussed below, where temperature is not given explicitly, it should be assumed to be 298 K.

Enthalpy. H ($= H_{298}^\circ$) for each individual species is defined according to eqn. (16).

$$H = H_0^\circ + (H_{298}^\circ - H_0^\circ) \quad (16)$$

where H_0° is the zero-point-corrected Born–Oppenheimer energy calculated from Gaussian 98, and adjusted as described above and shown in Fig. 1.

Entropy of mixing. Most species of interest here exist as mixtures of conformers and the entropy of mixing must be evaluated.³⁷ Enthalpies, H_i , and entropies, S_i , were used to calculate the free energy, G_i , for individual conformers, where

$$G_i = H_i - TS_i \quad (17)$$

The mole fraction, χ_i , for each is (eqn. (18)):

$$\chi_i = \frac{e^{-G_i/RT}}{\sum_{j=1}^n e^{-G_j/RT}} \quad (18)$$

The entropy of mixing, $S_{(\text{g})}^{\text{mix}}$, could then be calculated from eqn. (19),

$$S_{(\text{g})}^{\text{mix}} = -R \sum_{i=1}^n \chi_{(\text{g})i} \ln \chi_{(\text{g})i} \quad (19)$$

where n is the number of conformers.

Free energy ($G_{(\text{g})}$). The total free energy for a substance ($G_{(\text{g})}$) is given by eqn. (20).

$$G_{(\text{g})} = \sum_{i=1}^n G_{(\text{g})i} \chi_{(\text{g})i} - TS_{(\text{g})}^{\text{mix}} \quad (20)$$

This formulation of the free energy results in a single combined value for the reactants, transition states and products, each including the contributions from the different conformations. Free energies of reaction, ΔG , and free energies of activation, ΔG^\ddagger , are obtained by taking appropriate differences.

2.4. Solution phase

Solution models. Hydration energies³⁸ were calculated using two self-consistent reaction field (SCRf) models, COSMO³⁹ (conductor-like screening model) and SCIPCM⁴⁰ (self-consistent isodensity polarized continuum model). Within these models the solute is placed into a cavity surrounded by the solvent, defined as a continuum of uniform dielectric constant. The SCIPCM procedure defines the cavity as an isodensity (0.0004) surface of the electron density. The COSMO (or CPCM) procedure is parameterized using Hartree–Fock wavefunctions and a cavity constructed from united-atom radii.^{41,42} We have determined the CPCM free energies of solvation at the HF/6-31G(d,p) level, using united atom radii to define the cavities of the B3LYP/6-311+G(d,p)-optimized structures. CPCM provides an analysis of the total free energy of solvation, $\Delta G(\text{solv})$, in terms of a temperature-independent electrostatic interaction, $\Delta H(\text{es})$, and the temperature dependent nonelectrostatic contribution $\Delta G(\text{nes})$:

$$\Delta G(\text{solv}) = \Delta H(\text{es}) + \Delta G(\text{nes}) \quad (21)$$

The last term of eqn. (21), the “nonelectrostatic” in the G98 implementation, consists of three terms. Two of these, the dispersion and repulsion terms, are independent of temperature, and are here labelled $\Delta H(\text{dis})$ and $\Delta H(\text{rep})$, respectively. The temperature dependence of $\Delta G(\text{nes})$ arises solely in the third term, the free energy of cavity formation, $\Delta G(\text{cav})$, which, at 1 atm pressure is almost entirely due to the entropy of cavity formation, $\Delta S(\text{cav})$.⁴³

$$\Delta S(\text{cav}) = -(1/T)\Delta G(\text{cav}) \quad (22)$$

Thus one can write,

$$\Delta G(\text{solv}) = \Delta H(\text{solv}) - T\Delta S(\text{solv}) \quad (23)$$

where

$$\Delta H(\text{solv}) = \Delta H(\text{es}) + \Delta H(\text{dis}) + \Delta H(\text{rep}) \quad (24)$$

The SCIPCM model as implemented in G94, contains only electrostatic terms.^{40,42} In this model, $\Delta H(\text{solv})$ is taken as $\Delta H(\text{es})$.

In summary, the aqueous free energy, $G_{(\text{aq})i}$, of a component i of a mixture is given by eqn. (25),

$$G_{(\text{aq})i} = H_{(\text{g})i} + \Delta H(\text{solv})_i - TS_{(\text{g}\rightarrow\text{aq})i} - T\Delta S(\text{solv})_i \quad (25)$$

The entropy term, $S_{(\text{g}\rightarrow\text{aq})i}$, may simply be taken as $S_{(\text{g})i}$, or, as discussed below, modified to take into account aspects of the solution process not incorporated in continuum models.

For a given reaction in solution, the enthalpy of activation, $\Delta H_{(\text{aq})}^\ddagger$, is given by

$$\Delta H_{(\text{aq})}^\ddagger = \Delta H_{(\text{g})}^\ddagger + \Delta\Delta H(\text{solv}) \quad (26)$$

and the Arrhenius energy of activation, E_a , is given by⁴⁴

$$E_a = \Delta H_{(\text{aq})}^\ddagger + 2RT \quad (27)$$

Three solvation models. We utilize comparison to our experimental data to examine three approaches for the determination of free energies of solution, differing by the treatment of entropy changes upon solution, *i.e.*, $S_{(\text{g}\rightarrow\text{aq})i}$ (eqn. (25)). The approaches may be regarded as refinement of SCRf continuum solvation models, *e.g.*, COSMO, combined with TST for the determination of kinetic parameters for bimolecular reactions in solution. The most direct approach, *Solvation Model 1*, is to derive aqueous free energies by the simple expedient of addition of SCRf-derived $\Delta G(\text{solv})$ to gas phase $G_{(\text{g})}$ values, corrected to 1 mol dm⁻³.

$$G_{(\text{aq})} = G_{(\text{g})} + \Delta G(\text{solv}) \quad (28)$$

This approach is justified for continuum solvation models, like COSMO (invoked by CPCM in G98), because they are parameterized against experimental free energies for a test suite of molecules.⁴² However, it has been argued this procedure may greatly overestimate entropic effects.^{45,46} This is a serious concern when attempting to calculate free energies of activation for bimolecular reactions in solution, and is due to the fact that, in the gas phase, the major contributors to the entropy are the translational and rotational degrees of freedom which may be significantly reduced in solution due to specific solute-solvent interactions not incorporated into continuum models. In a bimolecular reaction, $A + B \rightarrow AB$, six translational and rotational degrees of freedom are converted to internal vibrations which are less subject to solvent interactions.

An alternative approach, *Solvation Model 2*, is to regard all gas-phase translational and rotational entropy as “lost” upon solution as the molecule (solute) is trapped in a solvent cage. This is tantamount to considering the solute and its solvation shell as a “supermolecule”. The gas-phase translational and rotational entropy would be replaced by an additional contribution from unspecified internal vibrations of the solute-solvent “supermolecule” cage. For *Solvation Model 2*, we adapt the procedure of Wolfe and coworkers, who derived the entropy, $S_{(\text{g}\rightarrow\text{aq})}$, of each solute by replacing the gas phase translational and rotational components of the entropy by the entropy 79.8 J mol⁻¹ K⁻¹, due to six vibrational modes with effective frequency, 115 cm⁻¹.⁴⁵ This effective frequency was derived non-empirically from a cage-like structure of water molecules surrounding the solute. We adopt this value although it was subsequently realized that some refinement was warranted.⁴⁶ In calculating the solution free energy of activation, the total $\Delta\Delta G(\text{solv})$ from COSMO, is incorporated into this model. This is also a departure from Wolfe and coworkers who used the single-spherical-cavity (Born) SCRf model.

Lastly, we examine a third, empirical approach, *Solvation Model 3*, in which we derive a part of the aqueous entropy, $S_{(\text{g}\rightarrow\text{aq})i}$, from experimental data as described below.

Entropy for solvation model 3: ($S_{(\text{aq})}$). Experimental gas phase entropies^{47,48} and entropies of solution are available for a number of substances,^{47,49} including three of the species

involved in this paper, namely, CH₄,⁴⁸ CH₃OH,⁴⁸ (CH₃)₂CHOH.⁴⁹ However, no experimental entropy data in aqueous solution are available for CH₃SH or any of the derived radicals, nor for the transition structures. We assume that the translational and rotational parts of the solution entropy of substances are the same if they are similar in shape and size, and derive the unknown solution entropies from the experimental values of related substances. Thus, we write the gas phase entropy, $S_{(\text{g})i}$, of a component, i , of a mixture of conformers in terms of its vibrational, electronic, and translational/rotational components, as

$$S_{(\text{g})i} = S_{(\text{g})}^{\text{vib}} + S_{(\text{g})}^{\text{elec}} + S_{(\text{g})}^{\text{trans,rot}} \quad (29)$$

and a parallel equation can be written for the aqueous phase entropy of i .

$$S_{(\text{aq})i} = S_{(\text{aq})}^{\text{vib}} + S_{(\text{aq})}^{\text{elec}} + S_{(\text{aq})}^{\text{trans,rot}} \quad (30)$$

The aqueous phase entropy of a substance, $S_{(\text{aq})}$, with n conformers is then given by:

$$S_{(\text{aq})} = S_{(\text{aq})}^{\text{vib}} + S_{(\text{aq})}^{\text{elec}} + S_{(\text{aq})}^{\text{trans,rot}} + R \ln n \quad (31)$$

where the last term approximates the entropy of mixing of the n conformers of similar populations.⁵⁰ The electronic contribution to the entropy is 0 for a singlet state and $R \ln 2$ for a doublet state, *i.e.*, a radical. We further assume that the vibrational and electronic parts of the entropy are the same for all conformers, and the same in the gas phase and in solution. Thus, the unknown aqueous entropy of one of our species $S_{(\text{aq})i}(\text{X})$, may be derived from the known experimental solution entropy, $S_{(\text{aq})i}(\text{X}')$ of a substance X' with n conformations by eqn. (32):

$$S_{(\text{aq})i}(\text{X}) = S_{(\text{aq})i}(\text{X}') - S_{(\text{g})}^{\text{vib}}(\text{X}') - R \ln n + S_{(\text{g})}^{\text{vib}}(\text{X}) + S_{(\text{g})}^{\text{elec}}(\text{X}) \quad (32)$$

In summary, the vibrational entropy of X' is calculated, and subtracted from its experimental solution entropy together with its entropy of mixing (if any), to be replaced by the calculated vibrational and electronic entropy of X . This procedure can be justified in part by the fact that solution entropies are largely independent of the mass of the solute.⁵¹ In the case of the transition structures, the solution entropy is derived from the most closely related stable molecule obtained by replacing the sulfur and central H atom by a CH₂CH₂ unit. Thus, the TS for the CH₃[•] + H-SCH₃ system is modelled by n-butane, for which the solution entropy is known. The models used for each system are presented in Table 1.

Table 1 The models and their experimental $S_{(\text{aq})}$ (J K⁻¹ mol⁻¹) values used in the derivation of the $S_{(\text{aq})}$ (J K⁻¹ mol⁻¹) for each species of interest

Model	$S_{(\text{aq})}(\text{exptl})^a$	Species modeled	$S_{(\text{aq})}(\text{calc})$
CH ₄	83.7 ^b	•CH ₃	97.5
CH ₃ OH	133.1 ^b	•CH ₂ OH	138.7
		CH ₃ SH	136.7
		CH ₃ S [•]	127.0
i-PrOH	154.8	•C(CH ₃) ₂ OH	156.1
Butane	167.2	TS1	176.3
n-Butanol	196.2	TS2a	195.4
		TS2b	197.3
3-Hexanol	234.3 ^c	TS3a	221.3
		TS3b	226.3
2-Methyl-2-butanol	182.2	TS3a	225.4
		TS3b	230.3

^a Calculated using gas phase entropies from ref. 48, and solvation entropies from ref. 49 unless noted otherwise. ^b Ref. 29. ^c Derived from calculated gas phase entropy, and solvation entropy from ref. 49.

Thus free energies of Solvation Model 3 are derived from eqn. (25), with $S_{(g \rightarrow aq)}$ replaced by $S_{(aq)}$. Two variations are considered, SM3a, and SM3b, depending upon whether $\Delta H(\text{solv})$ and $\Delta S(\text{solv})$ are obtained from CPCM or SCIPCM, respectively. In the case of SCIPCM, $\Delta S(\text{solv}) = 0$.

3. Experimental results and discussion

Using the approach described in Section 2.1, the rate constants of three α -hydroxyalkyl radicals ($\cdot\text{CH}_2\text{OH}$, $\cdot\text{CH}(\text{CH}_3)\text{OH}$, and $\cdot\text{C}(\text{CH}_3)_2\text{OH}$) and those of $\cdot\text{CH}_3$ and the less reactive primary alkyl radical $\cdot\text{CH}_2\text{C}(\text{CH}_3)_2\text{OH}$ have been determined by pulse radiolysis as a function of temperature.

The kinetics of the build up of the 390 nm absorption due to the disulfide radical anion (eqn. (8–10)) was biphasic. A small initial yield (within the first microseconds due to the interception of $\cdot\text{OH}$ and H^\cdot by 1,4-dithiothreitol) was followed by a much slower increase due to the reactions of the alkyl radicals with 1,4-dithiothreitol. The kinetics of this reaction was always of first order, and based on the 1,4-dithiothreitol concentration a bimolecular rate constant was calculated. Each data point represents a series of experiments at different doses per pulse. The data (not shown) were extrapolated to zero dose per pulse in order to eliminate artefacts by contributions of the second-order decay of the alkyl radicals. An Arrhenius plot is shown in Fig. 2. As is evident from the lines in Fig. 2, at all temperatures within the experimental range, 275 K–330 K, the order of the rates of reaction (1) ($\text{R}^\cdot\text{SH} = \text{dithiothreitol}$) is: $\cdot\text{C}(\text{CH}_3)_2\text{OH} > \cdot\text{CH}(\text{CH}_3)\text{OH} > \cdot\text{CH}_2\text{OH} > \cdot\text{CH}_3 > \cdot\text{CH}_2\text{C}(\text{CH}_3)_2\text{OH}$. A rationale is presented for this order after the theoretical results are presented and discussed.

From the data shown in Fig. 2, activation energies (E_a) and frequency factors (A) were calculated and are compiled in Table 2.

3.1. Theoretical results and discussion

Table 3 contains data for each individual species discussed in this study, including the isodesmic corrections to the enthal-

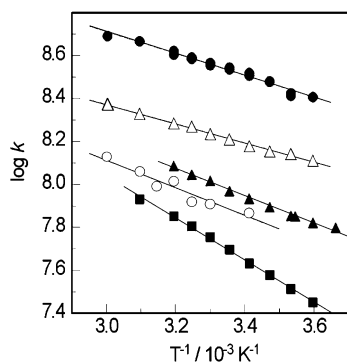


Fig. 2 Pulse radiolysis of N_2O -saturated solutions of 2-propanol (\bullet), ethanol (Δ), methanol (\blacktriangle), dimethylsulfoxide (\circ) and tertiary butanol (\blacksquare) ($0.05\text{--}0.3 \text{ mol dm}^{-3}$) in the presence of 1,4-dithiothreitol (1×10^{-3}). Arrhenius plots of the bimolecular rate constants of the reaction of the radicals with 1,4-dithiothreitol.

Table 2 Compilation of rate constants at 25°C , activation energies (E_a) and frequency factors (A) of some radicals with 1,4-dithiothreitol

Radical	k at $25^\circ\text{C}/\text{dm}^3 \text{ mol}^{-1} \text{ s}^{-1}$	Activation energy (E_a)/ kJ mol^{-1}	Frequency factor (A)
$\cdot\text{C}(\text{CH}_3)_2\text{OH}$	3.3×10^8	9.7	1.7×10^{10}
$\cdot\text{CH}(\text{CH}_3)\text{OH}$	1.5×10^8	8.6	0.52×10^{10}
$\cdot\text{CH}_2\text{OH}$	8.6×10^7	12.1	1.3×10^{10}
$\cdot\text{CH}_3$	7.4×10^7	12.3	1.1×10^{10}
$\cdot\text{CH}_2\text{C}(\text{CH}_3)_2\text{OH}$	4.3×10^7	18.7	9.5×10^{10}

pies, the tunnelling correction, the gas phase entropies, and total enthalpies and free energies of solution from CPCM and SCIPCM. The relative energies and the corresponding mole fractions (γ) for each species which are used to calculate their contribution to the total free energy, as well as in the calculation of S^{mix} , are given in Table 4. Table 5 summarizes the enthalpy and free energy results for each of the reactions as well as rate constants calculated at each level of treatment. In the first set of columns in Tables 4 and 5 under the heading, “Gas phase”, are gas phase results at 1 atm. The last set of columns under the heading “Solution phase” contain the results obtained by adding the CPCM and SCIPCM solution phase corrections, $\Delta\Delta H(\text{es})$, and $\Delta\Delta G(\text{nes})$, and incorporating $S_{(\text{aq})}$ from Table 1.

The transition states located for each reaction are shown in Fig. 3. One transition state (TS1) was located for the reaction with methyl radical, while two transition states (TS2a, TS2b and TS3a, TS3b) were located for each of the hydroxyalkyl radicals. In all cases the transition states involve a near linear attack ($\angle\text{C-H-S} \cong 175^\circ$). In the transition states, the C–H bond lengths are 0.578 \AA longer than that calculated for methane and an average of 0.470 \AA and 0.428 \AA longer than in methanol and 2-propanol, respectively. The S–H bond lengths in the transition states are only 0.087 \AA longer than that calculated for methanethiol for the reaction with methane and an average of 0.134 \AA and 0.156 \AA longer for the reaction with the hydroxymethyl radical and 2-hydroxy-2-propyl radical, respectively. These results are consistent with early transition states for these reactions.

Fig. 4 shows plots of the charges for each of the systems at the reactant, transition state and product points on the reaction coordinate. For each system the charges are summed into groups. Analysis of Fig. 4a for the reaction with methyl radical indicates that there is polarization in the transition state (TS1). The methanethio group takes on net negative charge in the transition state while the hydrogen and methyl groups take on positive charge. Fig. 4b shows an identical trend for the reaction with hydroxymethyl radical, only now the polarization has increased on each of the groups. This can only be due to the improved ability of the hydroxymethyl group to stabilize a positive charge over that of a methyl group. This trend continues for H-atom abstraction by 2-hydroxy-2-propyl radical (Fig. 4c).

Spin density analysis has been carried out, based on an AIM population analysis previously outlined by Wiberg *et al.*^{11,52} The spin density is defined as the difference in total α and β spins, separately integrated over the respective AIM atomic basins. The results are summarised in Fig. 5. Unlike the analysis of the charges which indicated that the charge polarization in the transition states was very different from that in the reactants or the products, the spins in the transition states appear to move quite directly to the final distribution in the products. Furthermore the spin density analysis confirms that the transition states are quite early, as would be expected, but could not be reflected in the charge polarization. Accordingly, in all three cases the spin density is still largely centered on the attacking radical.

Table 3 Total energies, zero point corrections, experimental corrections, tunneling factors, temperature corrections to the enthalpies, entropies in the gas phase as well as the solution phase free energy corrections from the CPCM and SCIPCM models for each species

Species	Gas phase							Solution phase		
	σ	$E/\text{hartree}$	ZPE/ kJ mol ⁻¹	$\Delta D/\text{kJ mol}^{-1}$	$\kappa/\text{kJ mol}^{-1}$	$H_{298}^{\circ} - H_0^{\circ}/\text{J K}^{-1} \text{mol}^{-1}$	$S^{\circ}/\text{kJ mol}^{-1}$	CPCM		SCIPCM ^b
								$\Delta H(\text{soln})/\text{kJ mol}^{-1}$	$\Delta G(\text{cav})/\text{kJ mol}^{-1}$	$\Delta H(\text{soln})^c/\text{kJ mol}^{-1}$
Radicals										
*CH ₃	6	-39.85517	77.8	7.3	—	10.5	194.6	-18.5	25.5	-1.8
*CH ₂ OH	1	-115.10249	97.3	10.7	—	11.4	241.1	-50.9	27.4	-16.0
*C(CH ₃) ₂ OH	1	-193.76814	246.2	10.7	—	17.5	309.0	-62.6	47.2	-13.1
CH ₃ S*	3	-438.10033	92.8	18.1	—	11.0	248.1	-40.2	36.1	-6.4
H*		-0.50216	—	—	—	—	—	—	—	—
Stable species										
CH ₄	12	-40.53393	116.9	—	—	10.0	186.1	-19.7	27.4	-0.6
CH ₃ OH	1	-115.76494	134.0	—	—	11.3	238.8	-51.8	28.8	-15.0
(CH ₃) ₂ CHOH(R1) ^d	1	-194.42425	282.2	—	—	17.1	299.2	-69.1	46.7	-13.5
(CH ₃) ₂ CHOH(R2) ^e	1	-194.42460	282.2	—	—	17.0	299.0	-68.6	46.5	-13.2
CH ₃ SH	1	-438.74322	120.4	—	—	12.0	253.9	-43.3	37.9	-7.6
Transition states										
TS1	1	-478.59609	200.3	10.0	1.19	18.1	329.6	-54.8	56.4	-9.2
TS2a	1	-553.84302	217.6	12.9	1.57	20.1	366.8	-85.7	59.8	-24.2
TS2b	1	-553.84373	217.7	12.9	1.53	20.1	368.7	-83.7	59.7	-22.6
TS3a	1	-632.50934	364.6	13.1	1.66	27.3	425.6	-98.3	77.8	-23.1
TS3b	1	-632.51034	364.4	13.1	1.58	27.6	430.3	-95.9	78.0	-18.9

^a Calculated at the ideal gas standard state (1 atm.). ^b SCIPCM values in italics were calculated using the 6-31+G(d) basis set. ^c Equal to $\Delta H(\text{es})$. ^d The *C* rotamer of 2-propanol. ^e The *C*₁ rotamer of 2-propanol.

Table 4 Relative energies^a and mole fractions in the gas phase and aqueous solution

Species	Gas phase				Solution phase ^b			
	n	ΔH	ΔG	χ	CPCM ^c		SCIPCM	
					ΔG	χ	ΔG	χ
(CH ₃) ₂ CHOH(R1) ^d	1	0.9	0.9	0.26	0.6	0.28	0.64	0.28
(CH ₃) ₂ CHOH(R2) ^e	2	0.0	0.0	0.37	0.0	0.36	0.0	0.36
TS2(a)	2	1.7	2.3	0.28	0.4	0.46	0.66	0.43
TS2(b)	2	0.0	0.0	0.72	0.0	0.54	0.0	0.57
TS3(a)	2	2.6	4.0	0.17	1.4	0.37	0.0	0.52
TS3(b)	2	0.0	0.0	0.83	0.0	0.63	0.2	0.48

^a Relative to the most stable conformation in each grouping. ^b Solution entropies taken from Table 1. ^c Including the $\Delta H(\text{soln})$ and $\Delta G(\text{cav})$ terms from CPCM (Table 3). ^d The *C*_s rotamer of 2-propanol. ^e The *C*₁ rotamer of 2-propanol.

Table 5 The enthalpies and free energies of reaction and activation (kJ mol⁻¹) at each level of treatment and the corresponding estimated rate constants (dm³ mol⁻¹ s⁻¹) for the reaction of C-centered radicals with methanethiol in the gas phase and aqueous solution

Radical	Gas phase ^a					Solution phase ^b									
	ΔH	ΔH^{\ddagger}	ΔG	ΔG^{\ddagger}	k	CPCM (SM3a)			SCIPCM (SM3b)						
						$\Delta H^{\ddagger c}$	$\Delta H^{\ddagger c}$	$\Delta G^{\ddagger d}$	$\Delta G^{\ddagger d}$	k^d	ΔH	ΔH^{\ddagger}	ΔG	ΔG^{\ddagger}	k
*CH ₃	-73.4	6.4	-67.2	41.9	8.5×10^6	-71.5	13.4	-64.4	23.7	5.3×10^8	-71.1	6.5	-64.1	23.8	5.0×10^8
*CH ₂ OH	-36.0	4.4	-30.0	42.2	9.4×10^6	-33.8	14.3	-27.8	32.4	2.0×10^7	-33.9	5.0	-27.6	28.5	9.7×10^7
*C(CH ₃) ₂ OH	-21.1	1.3	-15.5	41.1	1.5×10^7	-23.8	10.8	-24.3	23.5	7.8×10^8	-20.2	1.8	-17.9	21.8	1.5×10^9

^a Entropy calculated at the ideal gas standard state (1 atm.). ^b Solution entropies at the 1 mol dm⁻¹ standard state, taken from Table 1. ^c Including the $\Delta H(\text{soln})$ term from CPCM. ^d Including the $\Delta H(\text{soln})$ and $\Delta G(\text{cav})$ terms from CPCM.

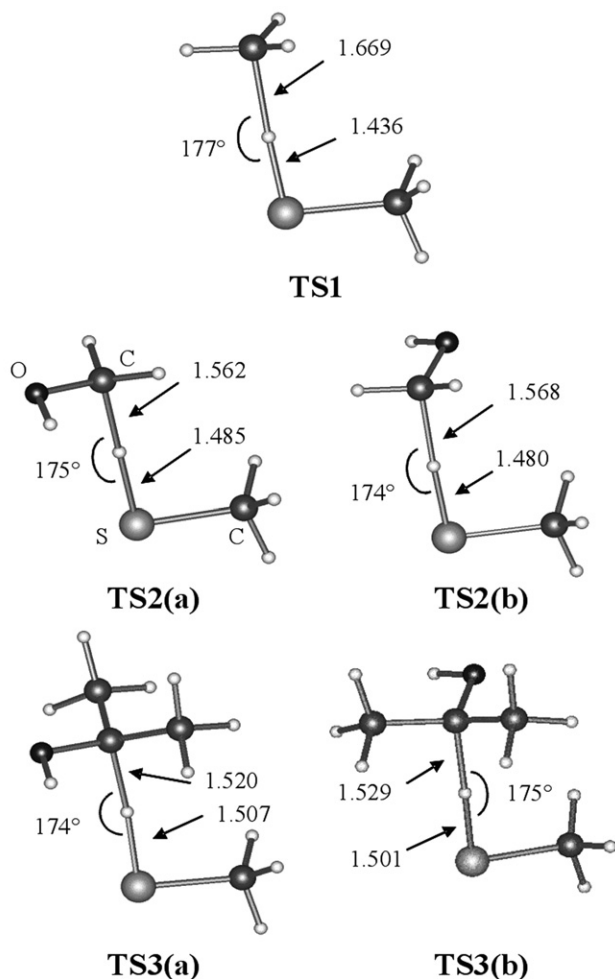
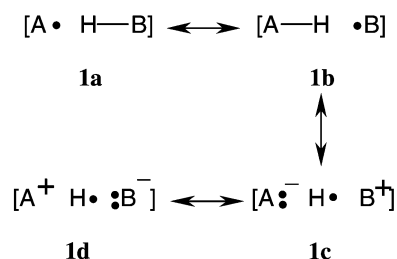


Fig. 3 Transition states for H-atom abstraction from methanethiol.

3.2. Gas phase

The gas phase enthalpy of reaction (1), ΔH , (Table 5) is exothermic with $\cdot\text{CH}_3 > \cdot\text{CH}_2\text{OH} > \cdot\text{C}(\text{CH}_3)_2\text{OH}$ in agreement with the decreasing BDE of the parents. However, the enthalpy of activation, ΔH^\ddagger , does not decrease with the increasing exothermicity of the reaction. While the differences are not large, the least stable radical, $\cdot\text{CH}_3$ has the highest ΔH^\ddagger , while the most stable, $\cdot\text{C}(\text{CH}_3)_2\text{OH}$, has the lowest ΔH^\ddagger . This trend can be understood in terms of a polarization model of the transition state as presented by Roberts and Steel.^{53,54} They have suggested that there are four key valence-bond structures (**1a-d**) which can be used to represent the transition state in a hydrogen atom transfer,



where **1c** might be better represented by **2a** and **2b** and likewise for **1d**.⁵³ These electronic configurations maximize the coulombic stabilization energy in the transition state.

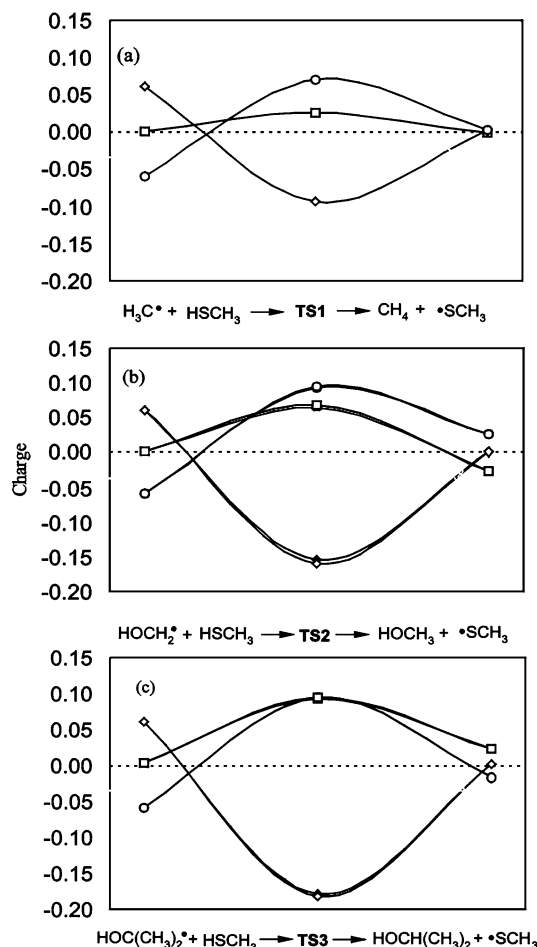
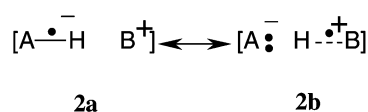


Fig. 4 Total AIM charges: (\square , \blacksquare), CH_3 , H_2COH or $(\text{CH}_3)_2\text{COH}$; (\diamond , \blacklozenge), SCH_3 ; (\circ , \bullet), central H atom. Open symbols represent curves containing **TS1**, **TS2a** and **TS3a** and filled symbols (partially hidden) represent curves containing **TS2b** and **TS2b**.

To the extent that the ionic resonance structures of the type **2a** and **2b** are important, the transition state will be stabilized and ΔH^\ddagger will be lower. In the present case, the A group corresponds to CH_3S and B corresponds to the CH_3 , CH_2OH or $\text{C}(\text{CH}_3)_2\text{OH}$ group. Analysis of the atomic charges, using AIMPAC,¹¹ suggests that the transition states examined here do benefit from this type of stabilization (Fig. 4). The polarization corresponds directly to valence bond configuration of type **2b**.⁵³ In order to maximize the so called “ionic resonance energy” (the polarization energy) the bulk of this positive charge resides on the hydrogen being transferred. This trend is exaggerated for the reaction with hydroxymethyl radical (Fig. 4b), resulting in increased stabilization in the transition state (**TS2a**, **TS2b**). This is due to the improved ability of the hydroxymethyl group to stabilize a positive charge over that of a methyl group. The trend continues for H-atom abstraction by 2-hydroxy-2-propyl radical (Fig. 4c). This increased polarization in the transition states ($\cdot\text{C}(\text{CH}_3)_2\text{OH} > \cdot\text{CH}_2\text{OH} > \cdot\text{CH}_3$) results in the observed enthalpies of activation (Table 5).

It may be noted here that Zavitsas^{55,56} favours an analysis of H-atom abstraction which emphasizes a triplet repulsion (anti-bonding) term due to a valence contributor of type **3** which must place parallel spins on A and B.



Commenting specifically on the reaction of C-centered radicals with thiols, Zavitsas has pointed out the sulfur and carbon

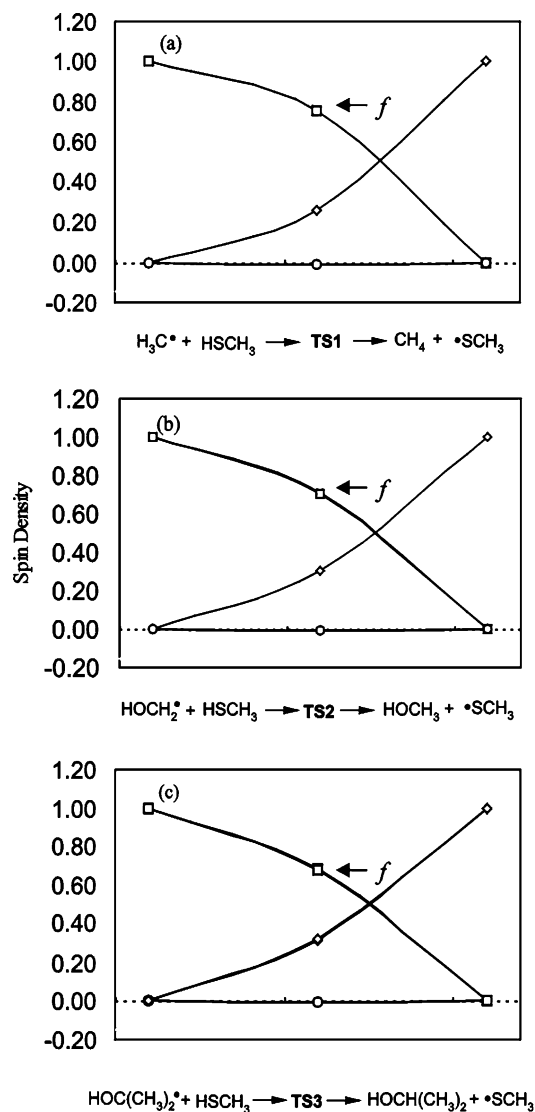


Fig. 5 Total AIM spin densities: (\square , \blacksquare), CH_3 , H_2COH or $(\text{CH}_3)_2\text{COH}$; (\diamond , \blacklozenge), SCH_3 ; (\circ , \bullet), central H atom. Open symbols represent curves containing **TS1**, **TS2a** and **TS3a** and filled symbols (partially hidden) represent curves containing **TS2b** and **TS3b**. Fraction of the spin, f , on the C-centered fragment in the transition state: CH_3 , $f = 0.75$; H_2COH , $f = 0.7$; $(\text{CH}_3)_2\text{COH}$; $f = 0.67$.

have similar electronegativities suggesting that such criteria would offer little guidance to the direction of the charge polarization in the transition state. To the extent that resonance structure **3** is important, it requires similar fractions of spin on the C and S centers. However, our spin density analysis (Fig. 5) indicates that the spin is very unequally distributed in the TS ($f = 0.67 - 0.75$). In fact **TS3** which has the spin the most evenly distributed over the A and B groups, presumably resulting in the highest triplet repulsion, actually has the lowest ΔH^\ddagger .

The observed differences in the enthalpy of activation can also be understood in terms of orbital interaction theory.^{12,13} The important interaction is between the LUMO of methanethiol and the SOMO of each C-centered radical (Fig. 6). The SOMO energies increase in the order ${}^{\bullet}\text{CH}_3 < {}^{\bullet}\text{CH}_2\text{OH} < {}^{\bullet}\text{C}(\text{CH}_3)_2\text{OH}$ resulting in a stronger interaction for the higher energy SOMOs with the σ^* orbital of the H-S bond. This stronger interaction results in an increased stabilization of the transition state (Table 5).

The picture is a little different once the gas phase entropy is factored in to give the free energy of reaction and activation (ΔG and ΔG^\ddagger , Table 5). Although ΔG and ΔH hold the same

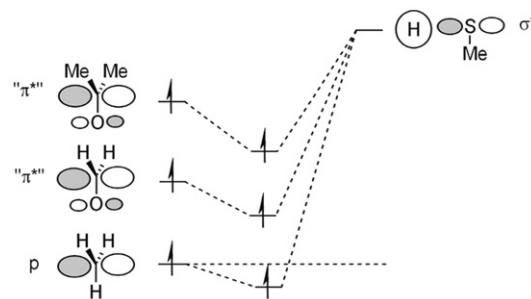


Fig. 6 Orbital interaction analysis of the H-atom abstraction from methanethiol by the three C-centered radicals.

trend, this is not true for ΔH^\ddagger and ΔG^\ddagger . The relative differences in ΔG^\ddagger from one reaction to the next are less than for ΔH^\ddagger . This is due to the loss of translational and rotational entropy ($S^{\text{trans,rot}}$) to vibrational entropy (S^{vib}) as the reactants move along the reaction coordinate towards the transition state. Since this loss in entropy is greatest for the most massive reactants, the methyl radical system loses the least entropy.

Several experimental gas phase rate data are available for the reaction of methyl radical with thiols.⁵⁷⁻⁵⁹ The most recent determination, $k = 5 \times 10^6 \text{ dm}^3 \text{ mol}^{-1} \text{ s}^{-1}$ (${}^{\bullet}\text{CH}_3 + \text{HSC}_2\text{H}_5$ at 298 K),⁵⁸ is in good agreement with our calculated gas phase value of $k = 8.5 \times 10^6 \text{ dm}^3 \text{ mol}^{-1} \text{ s}^{-1}$ (Table 5), but suggests that our activation enthalpy may be a little too low.

3.3. Solution phase

Enthalpy in solution. The electrostatic component of the energy of solvation, $\Delta H(\text{solv}) (= \Delta H(\text{es}))$, derived from SCIPCM is given for each species in the last column of Table 2. The enthalpy changes for reaction (1) (see Table 5) ($\text{R}^{\bullet}\text{SH} = \text{CH}_3\text{SH}$) due to solvation, $\Delta H(\text{es})$, represent modest increases in ΔH of reaction (in kJ mol^{-1}): ${}^{\bullet}\text{CH}_3$, +2.3; ${}^{\bullet}\text{CH}_2\text{OH}$, +2.1; ${}^{\bullet}\text{C}(\text{CH}_3)_2\text{OH}$, +0.9. In other words, the exothermicity of the reaction in the gas phase (Table 5, column 2) is reduced by these amounts in solution. The effect on the enthalpy of activation, ΔH^\ddagger , is even less ($\Delta\Delta H^\ddagger(\text{es})$ in kJ mol^{-1}): ${}^{\bullet}\text{CH}_3$, +0.1; ${}^{\bullet}\text{CH}_2\text{OH}$, +0.1; ${}^{\bullet}\text{C}(\text{CH}_3)_2\text{OH}$, +0.5. The $\Delta\Delta H^\ddagger(\text{es})$ values derived by CPCM are very similar (data not shown), but in the CPCM case, $\Delta H(\text{solv})$ includes the temperature-independent components of $\Delta G(\text{es})$. The predicted aqueous enthalpies of activation are significantly higher than the gas phase values, $\Delta\Delta H^\ddagger(\text{solv})$: ${}^{\bullet}\text{CH}_3$, +7.0; ${}^{\bullet}\text{CH}_2\text{OH}$, +9.9; ${}^{\bullet}\text{C}(\text{CH}_3)_2\text{OH}$, +9.5. The negligibly small effect by SCIPCM, and positive effect by CPCM, on the enthalpy of activation due to immersion in the polar solvent (water) are somewhat surprising in view of the afore-mentioned charge polarization in the TS.

Free energy in solution. According to *Solvation Model 1* (eqn. (28)), free energies of reaction and activation may be derived by simply adding the appropriate $\Delta\Delta G(\text{solv})$ to gas-phase ΔG values. By CPCM, $\Delta\Delta G(\text{solv})$ values for the free energy of activation are (in kJ mol^{-1}): CH_3^{\bullet} , 0.0; $\text{H}_2\text{C}^{\bullet}\text{OH}$, +4.1; $(\text{CH}_3)_2\text{C}^{\bullet}\text{OH}$, +1.8. Thus a modest slowing down of the reaction from the gas phase rate is predicted. The rate constants predicted by *Solvation Model 1* are compared to the experimentally determined values in Table 6. All reactions are predicted to be slower than observed, by factors of 8.7, 57, and 61 for ${}^{\bullet}\text{CH}_3$, ${}^{\bullet}\text{CH}_2\text{OH}$, and ${}^{\bullet}\text{C}(\text{CH}_3)_2\text{OH}$, respectively. The discrepancy is worse for the larger systems, as previously noted, and is attributed to improper accounting of the exchange of gas-phase rotational and translational entropy for vibrational entropy in solution.⁴⁵ *Solvation Model 2* represents an attempt to account for this by application of

Table 6 Comparison of k and E_a from different solvation models (25 °C)^a

Radical	$k/10^7 \text{ dm}^3 \text{ mol}^{-1} \text{ s}^{-1}$					$E_a/\text{kJ mol}^{-1}$		
	SM1	SM2	SM3a	SM3b	exptl	SM3a	SM3b	exptl
$\cdot\text{CH}_3$	0.85	4.9×10^3	53	50	7.4	18.4	11.5	12.3
$\cdot\text{CH}_2\text{OH}$	0.15	8×10^3	2.0	9.7	8.6	19.3	10.0	12.1
$\cdot\text{C}(\text{CH}_3)_2\text{OH}$	0.54	3.9×10^5	78	150	33	15.8	6.8	9.7

^a Solvation Models 1, 2, and 3 = SM1, SM2, and SM3 (see text).

vibrational entropy due to six modes with an effective frequency, 115 cm^{-1} . However, this procedure yields rates which are too fast by 3 to 4 orders of magnitude (Table 6). Evidently the entropy change is not large enough. While closer agreement with experiment may be achieved by choosing a lower frequency, we have not pursued this route. It is clear a rational manner of determining entropies in solution is required.

Entropy in solution (S_{aq}). A number of approaches to the problem of calculating entropies of substances in solution have been proposed in the past. However they either have not been parameterized^{60–63} for systems similar to those of interest here or perform poorly for systems of this size.⁴⁵ In any case S_{aq} is a macroscopic property depending on both the solvent and the solute and any attempt to parameterize information calculated at a molecular level will be in some sense artificial.

Table 1 contains the solution entropies (S_{aq}) as calculated by our entropy model procedure described in Section 2.4. Although the S_{aq} values (Table 1) are dramatically smaller than the S_{g} values (Table 3) for each individual species, the free energies of activation derived using S_{aq} are 18.0 kJ mol^{-1} , 13.7 kJ mol^{-1} and 19.3 kJ mol^{-1} lower for the $\cdot\text{CH}_3$, $\cdot\text{CH}_2\text{OH}$ and $\cdot\text{C}(\text{CH}_3)_2\text{OH}$ systems respectively than the values derived from S_{g} . In each case a constant portion of this free energy change, 7.9 kJ mol^{-1} , is simply a result of the change in the entropy due to the concentration difference between the ideal gas standard state (1 atm) and the 1 mol dm^{-3} standard state in solution.

Solvation Model 3 attempts to determine an effective entropy in solution for each species by replacing the gas-phase translational and rotational components with the solution quantity obtained by extrapolation from experimental entropies in solution of related species. Free energies are determined by eqn. (25), which includes contributions from the standard continuum models, CPCM (SM3a) and SCIPCM (SM3b). The rates predicted by both SM3a and SM3b are compared in Table 6 to the experimental rates. Both methods yield rates for the two hydroxy radicals which are in the right order and within a factor of 4 or 5 of the experimental values. In the case of SM3b, the methyl radical is slightly slower than in SM3a, and the hydroxyalkyl radicals are faster, improving the agreement of $\cdot\text{CH}_2\text{OH}$ with experiment, but making the absolute agreement for $\cdot\text{C}(\text{CH}_3)_2\text{OH}$ somewhat worst.

Arrhenius activation energy, E_a . The Arrhenius activation energy, E_a , provides a sensitive additional determinant of the validity of the procedures employed and does not depend on the accuracy of the estimated entropy changes. E_a values were calculated by eqns. (26) and (27), and are compared to the experimental values in Table 6. Solvation models SM1, SM2, and SM3a all employ CPCM values and yield almost identical E_a values. Only those for SM3a are shown in Table 6. For each of the radicals, the calculated E_a values for SM3a are 6 to 7 kJ mol^{-1} too high compared to the experimental values. While in an absolute sense, this is a small error, the values derived by SM3b which employs SCIPCM solution values, are closer still, being uniformly lower than experimen-

tal but deviating by less than 3 kJ mol^{-1} and showing the same trend as the experimental results. The success of SM3b is remarkable since the SCIPCM procedure contains no short range dispersion and repulsion terms.

4. Conclusions

The Arrhenius parameters and rates of reaction of three hydroxyl radicals, methyl radical, and the hindered primary C-centred radical from t-butyl alcohol with dithiothreitol were measured by pulse radiolysis in water. The bimolecular rate constants were found to be in the order: $\cdot\text{C}(\text{CH}_3)_2\text{OH} > \cdot\text{CH}(\text{CH}_3)\text{OH} > \cdot\text{CH}_2\text{OH} > \cdot\text{CH}_3 > \cdot\text{CH}_2\text{C}(\text{CH}_3)_2\text{OH}$. The reaction of three of these, $\cdot\text{C}(\text{CH}_3)_2\text{OH}$, $\cdot\text{CH}_2\text{OH}$, and $\cdot\text{CH}_3$, with methanethiol were examined with high-level quantum chemical calculations, coupled with transition state theory, both in the gas phase and in solution. The steric effects which contribute to the slow rate of reaction of $\cdot\text{CH}_2\text{C}(\text{CH}_3)_2\text{OH}$ were not examined. Analysis of the atomic charges indicates that the observed order of reactivity and ΔH^\ddagger , which are contrary to the BDE of the radical's parents, can be understood in terms of increasing polarization in the transition states ($\cdot\text{C}(\text{CH}_3)_2\text{OH} > \cdot\text{CH}_2\text{OH} > \cdot\text{CH}_3$). Polarization of the transition state appears to result in an "ionic resonance energy" stabilization consistent with the proposals of Roberts and Steel.⁵³ The order is also readily understandable by orbital interaction theory as being determined by SOMO–LUMO (σ_{SH}^*) interactions. Standard continuum models of solvation, COSMO and SCIPCM, were applied to examine the effect of solvent on the calculated rates of reaction. It is verified that special consideration must be given to entropy changes upon solution. Good agreement with experiment could be achieved with both continuum models if the aqueous entropy was derived by extrapolation from experimental values of model systems. SCIPCM yielded better agreement with experiment against the criteria of both the rate constants and Arrhenius activation energies.

Acknowledgements

The financial assistance of the Natural Sciences and Engineering Council of Canada (NSERC) is gratefully acknowledged.

References

- 1 C. von Sonntag, *The Chemical Basis of Radiation Biology*, Taylor & Francis, London, 1987, pp. 353–374.
- 2 M. D. Haque and B. P. Roberts, *Tetrahedron Lett.*, 1996, **37**, 9123–9126.
- 3 P. Wardman and C. von Sonntag, *Methods Enzymol.*, 1995, **251**, 31–45.
- 4 L. A. Moran, K. G. Scrimgeour, H. R. Horton, R. S. Ochs and J. D. Rawn, *Biochemistry*, Neil Patterson Publ., Prentice Hall, Englewood Cliffs, NJ, 2nd edn., 1994.
- 5 N. Takahashi and T. E. Creighton, *Biochemistry*, 1996, **35**, 8342–8353.

- 6 J. Stubbe and W. A. van der Donk, *Chem. Rev.*, 1998, **98**, 705–762.
- 7 W. Karmann, A. Granzow, G. Meissner and A. Henglein, *Int. J. Radiat. Phys. Chem.*, 1969, **1**, 395–405.
- 8 J. L. Redpath, *Radiat. Res.*, 1973, **54**, 364–374.
- 9 G. E. Adams, G. S. McNaughton and B. D. Michael, *Trans. Faraday Soc.*, 1968, **64**, 902–910.
- 10 M. S. Akhlaq and C. von Sonntag, *J. Am. Chem. Soc.*, 1986, **108**, 3542–3544.
- 11 R. F. W. Bader, *Atoms in Molecules. A Quantum Theory*, Clarendon, Oxford, 1990.
- 12 A. Rauk, *Orbital Interaction Theory of Organic Chemistry*, John Wiley & Sons, Inc., Toronto, 2nd edn., 2001.
- 13 I. Fleming, *Frontier Orbitals and Organic Chemical Reactions*, John Wiley & Sons, Toronto, 1990.
- 14 C. von Sonntag and H.-P. Schuchmann, *Methods Enzymol.*, 1994, **233**, 3–20.
- 15 G. V. Buxton, C. L. Greenstock, W. P. Helman and A. B. Ross, *J. Phys. Chem. Ref. Data*, 1988, **17**, 513–886.
- 16 K.-D. Asmus, H. Möckel and A. Henglein, *J. Phys. Chem.*, 1973, **77**, 1218–1221.
- 17 H.-P. Schuchmann and C. von Sonntag, *J. Photochem.*, 1981, **16**, 289–295.
- 18 M. Erben-Russ, W. Bors and M. Saran, *Int. J. Radiat. Biol.*, 1987, **52**, 393–412.
- 19 D. Veltwisch, E. Janata and K.-D. Asmus, *J. Chem. Soc., Perkin Trans. 2*, 1980, 146–153.
- 20 M. S. Akhlaq and C. von Sonntag, *Z. Naturforsch.*, 1987, **42c**, 134–140.
- 21 P. C. Chan and B. H. J. Bielski, *J. Am. Chem. Soc.*, 1973, **95**, 5504–5508.
- 22 M. J. Frisch, G. W. Trucks, H. B. Schlegel, G. E. Scuseria, M. A. Robb, J. R. Cheeseman, V. G. Zakrzewski, J. A. Montgomery, Jr., R. E. Stratmann, J. C. Burant, S. Dapprich, J. M. Millam, A. D. Daniels, K. N. Kudin, M. C. Strain, O. Farkas, J. Tomasi, V. Barone, M. Cossi, R. Cammi, B. Mennucci, C. Pomelli, C. Adamo, S. Clifford, J. Ochterski, G. A. Petersson, P. Y. Ayala, Q. Cui, K. Morokuma, D. K. Malick, A. D. Rabuck, K. Raghavachari, J. B. Foresman, J. Cioslowski, J. V. Ortiz, A. G. Baboul, B. B. Stefanov, A. Liashenko, P. Piskorz, I. Komaromi, R. Gomperts, L. R. Martin, D. J. Fox, T. Keith, M. A. Al-Laham, C. Y. Peng, A. Nanayakkara, C. Gonzalez, M. Challacombe, P. M. W. Gill, B. Johnson, W. Chen, M. W. Wong, J. L. Andres, C. Gonzalez, M. Head-Gordon, E. S. Replogle and J. A. Pople, *Gaussian 98, Revision A.7*, 1998, Gaussian, Inc., Pittsburgh PA.
- 23 M. J. Frisch, G. W. Trucks, H. B. Schlegel, P. M. W. Gill, B. G. Johnson, M. A. Robb, J. R. Cheeseman, T. Keith, G. A. Petersson, J. A. Montgomery, K. Raghavachari, M. A. Al-Laham, V. G. Zakrzewski, J. V. Ortiz, J. B. Foresman, D. Y. Peng, P. Y. Ayala, W. Chen, M. W. Wong, J. L. Andres, E. S. Replogle, R. Gomperts, R. L. Martin, D. J. Fox, J. S. Binkley, D. J. Defrees, J. Baker, J. P. Stewart, M. Head-Gordon, C. Gonzalez and J. A. Pople, *Gaussian 94, Revision B.3*, Gaussian, Inc., Pittsburgh, PA, 1995.
- 24 A. P. Scott and L. Radom, *J. Phys. Chem.*, 1996, **100**, 16502–16513.
- 25 N. Kobko and J. J. Dannenberg, *J. Phys. Chem. A*, 2001, **105**, 1944–1950.
- 26 J. D. Cox and D. D. Wagman and V. A. Medvedev, *CODATA Key Values for Thermodynamics*, Hemisphere, New York, NY, 1989.
- 27 J. Berkowitz, G. B. Ellison and D. Gutman, *J. Phys. Chem.*, 1994, **98**, 2744–2765.
- 28 J. P. Pedley, R. D. Naylor, and S. P. Kirby, *Thermodynamic Data of Organic Compounds*, Chapman and Hall, New York NY, 2nd edn., 1986.
- 29 M. W. Chase, C. A. Davies, J. R. Downey, Jr., D. J. Frurip, R. A. McDonald and A. N. Syverud, *JANAF Thermodynamic Tables*, 3rd edn., *J. Phys. Chem. Ref. Data, Suppl. 1*, 1985, **14**, 1–1856.
- 30 R. D. Johnson III and J. W. Hudgens, *J. Phys. Chem.*, 1996, **100**, 19874–19890.
- 31 R. Atkinson, D. L. Baulch, R. A. Cox, R. F. Hampson, Jr., J. A. Kerr, M. J. Rossi and J. Troe, *J. Phys. Chem. Ref. Data*, 1997, **26**, 1329–1499.
- 32 G. K. Vemulapalli, *Physical Chemistry*, Prentice Hall, Englewood Cliffs, NJ, 1993.
- 33 E. P. Wigner, *Z. Phys. Chem., Abt. B*, 1932, **19**, 203.
- 34 H. S. Johnston, *Gas Phase Reaction Rate Theory*, Ronald Press, New York, 1966.
- 35 B. C. Garrett and D. G. Truhlar, *J. Phys. Chem.*, 1979, **83**, 200–203.
- 36 D. A. McQuarrie, *Statistical Thermodynamics*, Harper & Row, New York, NY, 1973.
- 37 S. W. Benson, *Thermochemical Kinetics, Methods for the Estimation of Thermochemical Data and Rate Parameters*, John Wiley & Sons, Toronto, 2nd edn., 1976.
- 38 Strictly speaking, hydration energies are free energies. However, we treat the temperature-independent components of free energies of solvation as enthalpies.
- 39 (a) A. Klamt and G. Schüürmann, *J. Chem. Soc., Perkin Trans. 2*, 1993, 799–805; (b) J. Andzelm, C. Kolmel and A. Klamt, *J. Chem. Phys.*, 1995, **103**, 9312–9320.
- 40 J. B. Foresman, T. A. Keith, K. B. Wiberg, J. Snoonian and M. J. Frisch, *J. Phys. Chem.*, 1996, **100**, 16098–16104.
- 41 R. Arnaud, C. Adamo, M. Cossi, A. Milet, Y. Vallee and V. Barone, *J. Am. Chem. Soc.*, 2000, **122**, 324–330.
- 42 V. Barone, M. Cossi and J. Tomasi, *J. Chem. Phys.*, 1997, **107**, 3210–3221.
- 43 R. A. Pierotti, *Chem. Rev.*, 1976, **76**, 717–726.
- 44 P. J. Robinson, *J. Chem. Ed.*, 1978, **55**, 509–510.
- 45 S. Wolfe, C.-K. Kim, K. Yang, N. Weinberg and Z. Shi, *J. Am. Chem. Soc.*, 1995, **117**, 4240–4260.
- 46 S. Wolfe, Z. Shi, K. Yang, S. Ro, N. Weinberg and C.-K. Kim, *Can. J. Chem.*, 1998, **76**, 114–124.
- 47 D. D. Wagmen, W. H. Evans, V. B. Parker, R. H. Schumm, I. Halow, S. M. Bailey, K. L. Churney and R. L. Nuttall, *J. Phys. Chem. Ref. Data*, 1982, **11**, Suppl. No. 2.
- 48 D. R. Stull, E. F. Westrum, Jr. and G. C. Sinke, *The Chemical Thermodynamics of Organic Compounds*, John Wiley & Sons, New York, NY, 1969.
- 49 S. Cabani, P. Gianni, V. Mollica and L. Lepori, *J. Solution Chem.*, 1981, **10**, 563–595.
- 50 J. P. Guthrie, *J. Phys. Chem. A*, 2001, **105**, 8495–8499.
- 51 B. C. Garrett and G. K. Schenter, *Nonequilibrium Solvation for an Aqueous-Phase Reaction*, in *Structure and Reactivity in Aqueous Solution*, ed. J. C. Cramer and D. G. Truhlar, American Chemical Society, Washington, 1994, pp. 122–142.
- 52 K. B. Wiberg, J. R. Cheeseman, J. W. Ochterski and M. J. Frisch, *J. Am. Chem. Soc.*, 1995, **117**, 6535–6543.
- 53 B. P. Roberts and A. J. Steel, *J. Chem. Soc., Perkin Trans. 2*, 1994, 2155–2162.
- 54 B. P. Roberts, *J. Chem. Soc., Perkin Trans. 2*, 1996, 2719–2725.
- 55 A. A. Zavitsas and C. Chatgililoglu, *J. Am. Chem. Soc.*, 1995, **117**, 10645–10654.
- 56 A. A. Zavitsas, *J. Chem. Soc., Perkin Trans. 2*, 1996, 391–393.
- 57 J. A. Kerr and A. F. Trotman-Dickenson, *J. Chem. Soc.*, 1957, 3322.
- 58 G. Lenvag and T. Berces, *J. Photochem. A*, 1987, **40**, 31.
- 59 G. Greig and J. C. Thynne, *Trans. Faraday Soc.*, 1966, **62**, 379–387.
- 60 D. H. Wertz, *J. Am. Chem. Soc.*, 1980, **102**, 5316–5322.
- 61 M. H. Abraham, *J. Am. Chem. Soc.*, 1981, **103**, 6742–6744.
- 62 I. H. Williams, *J. Am. Chem. Soc.*, 1987, **109**, 6299–6307.
- 63 J. Florián and A. Warshel, *J. Phys. Chem. B*, 1999, **103**, 10282–10288.